Development 137, 2253-2264 (2010) doi:10.1242/dev.032409

Modelling the Bicoid gradient

Oliver Grimm[1,*,†], Mathieu Coppey[2,*,†] and Eric Wieschaus[1,†]

Summary

Morphogen gradients provide embryonic tissues with positional information by inducing target genes at different concentration thresholds and thus at different positions. The Bicoid morphogen gradient in *Drosophila melanogaster* embryos has recently been analysed quantitatively, yet how it forms remains a matter of controversy. Several biophysical models that rely on production, diffusion and degradation have been formulated to account for the observed dynamics of the Bicoid gradient, but no one model can account for all its characteristics. Here, we discuss how existing data on this gradient fit the various proposed models and what aspects of gradient formation these models fail to explain. We suggest that knowing a few additional parameters, such as the lifetime of Bicoid, would help to identify and develop better models of Bicoid gradient formation.

Key words: Bicoid, Morphogen, Pattern formation

Introduction

A fundamental question in developmental biology is how naïve tissue is provided with positional information. One answer to this question posed the idea of morphogens (Turing, 1952), pattern-generating substances that form concentration gradients across fields of cells (Wolpert, 1969; Crick, 1970; Gierer and Meinhardt, 1972). Simple molecular mechanisms, such as localised protein synthesis, diffusion and degradation, can yield non-uniform distributions of morphogens that determine pattern formation. In the modern formulation, cells or nuclei would respond to different concentration thresholds of the morphogen by the expression of specific target genes, thereby translating the differential morphogen concentration into patterns of gene expression (Wolpert, 1969; Crick, 1970).

The simplicity of the morphogen gradient model has been attractive to developmental biologists in that it reduces the problem of specifying positional information to measuring quantitative differences in a single molecule. It is relatively easy to envision cell biological processes and signalling events that could localise a morphogen source or break symmetry. The final information-rich distribution of a morphogen is controlled by measurable physical parameters, such as diffusion and lifetime.

bicoid, which encodes a homeobox transcription factor, was the first gene to be identified that fulfils the criteria of such a morphogen. The Bicoid gradient arises from maternally deposited mRNA at the anterior pole of the syncytial *Drosophila* embryo (St Johnston et al., 1989). It is translated at the start of egg deposition, and its protein gradient is established in less than 3 hours and is subsequently read by ~20 target genes, which are expressed in discrete patterns along the anterior-posterior (AP) axis (Jaeger et al., 2004; Schroeder et al., 2004; Ochoa-Espinosa et al., 2005; Manu et al., 2009a; Manu et al., 2009b; Ochoa-Espinosa et al., 2009).

A number of other morphogens were identified following the discovery of Bicoid. These include members of the Fibroblast growth factor (FGF), Transforming growth factor β (TGFβ), Hedgehog and Wingless (Wg) families, which pattern a wide variety of tissues in many different animals (Tabata and Takei, 2004). The biophysical parameters of several of these morphogens have also been measured; for example, for Decapentaplegic (Dpp; which belongs to the TGFβ family) and for Wg in the wing disk epithelium of *Drosophila* (Kicheva et al., 2007), for Fgf8 in the zebrafish embryo (Yu et al., 2009) and for the transcription factor Dorsal (Dl; the homologue of nuclear factor kappa B, NFκB) and Mitogen-activated protein kinase (MAPK) in the syncytial *Drosophila* embryo (DeLotto et al., 2007; Coppey et al., 2008; Kanodia et al., 2009). Lessons obtained from any of these gradients are potentially informative about the formation of morphogen gradients in general, but each gradient is distinguished by its own special features. In this review, we focus on the Bicoid gradient, which is the most thoroughly studied morphogen gradient. Our aim is to introduce the major classes of models and to discuss how quantitative data recently obtained from living embryos (Box 1) fit with each model, and which features of the Bicoid gradient are inconsistent with each model's predictions. We conclude by suggesting that knowing more about additional parameters of this gradient would help us to understand which of the models, if any, most accurately describes the formation of the Bicoid gradient and how future models could be improved.

Analysing the Bicoid gradient

Since its discovery in 1988, the Bicoid gradient has been analysed by a multitude of methods (Ephrussi and St Johnston, 2004). For the purpose of this review, we focus on those findings that directly relate to the biophysical models that we discuss.

bicoid RNA begins to be translated at egg deposition at a rate that is generally believed to be constant, and the protein gradient is established in less than 3 hours in the syncytial embryo, which is ~500 μm in length (Fig. 1, Fig. 2A). The protein is thought to move from its site of production to form a nuclear concentration gradient: nuclei closer to the source at the anterior contain higher concentrations of Bicoid than nuclei posterior to this position (Fig. 1, Fig. 2A,B). The environment in which the Bicoid gradient forms is highly dynamic and heterogeneous (Fig. 1). Following fertilisation, the embryo undergoes 13 synchronous rounds of nuclear division, such that within 2 hours the number of nuclei in the embryo increases by three orders of magnitude, from 1 to ~6000 nuclei [the nuclear diameter is ~10 μm until cycle 10, and then decreases to ~6 μm in cycle 14 (Gregor et al., 2007a)] (Fig. 1). In cycle 14, nuclei occupy ~30% of the cortical area that is

[1]Howard Hughes Medical Institute, Department of Molecular Biology, Princeton University, Princeton, NJ 08544, USA. [2]Laboratoire Kastler Brossel, Ecole normale supérieure, 46, rue d'Ulm, 75005 Paris, France.

*These authors contributed equally to this work
†Authors for correspondence (ogrimm@princeton.edu; coppey@biologie.ens.fr; efw@princeton.edu)

Box 1. Quantitative measurements of the Bicoid gradient

The recent reanalysis of the Bicoid gradient using live imaging of an enhanced green fluorescent protein (EGFP)-tagged form of Bicoid (Gregor et al., 2005; Gregor et al., 2007a; Gregor et al., 2007b) has allowed the dynamics of gradient formation to be followed quantitatively in living *Drosophila* embryos. The major findings from these and other recent studies that must be accounted for in the models of Bicoid gradient formation are as follows:

- The intranuclear concentration gradient of Bicoid is well approximated by an exponentially decaying concentration profile (Driever and Nusslein-Volhard, 1988a; Houchmandzadeh et al., 2002; Gregor et al., 2007a). This gradient is established within 90 minutes or less (Gregor et al., 2007a).
- Bicoid diffuses relatively slowly (D=0.3 μm^2/second) in the cortical cytoplasm on a time scale of minutes (Gregor et al., 2007a).
- The nuclear Bicoid gradient is stable over cell cycles 10-14. In particular, the initial concentration in nuclei in successive cycles is constant to within 10%, even though it decays by ~30% during the subsequent interphase period as nuclear volume and surface area change (Gregor et al., 2007a).
- Nuclear Bicoid is in a dynamic equilibrium, which is brought about by its rapid import and export between the cytoplasm and the nucleus (Gregor et al., 2007a).
- The spatial shape of the Bicoid gradient (the length constant for an exponential decay) scales with embryo length over a factor of five in different dipteran species with different egg sizes (Gregor et al., 2005).

thought to be available for the movement of Bicoid. The first ten nuclear cycles last on average 8 minutes each, followed by a slowing of the cell cycle [9.5, 12, 21 and 60 minutes for cycles 11, 12, 13 and 14, respectively (Foe and Alberts, 1983)]. The egg is initially a homogeneous mixture of yolk granules and cytoplasmic material surrounding the syncytial nuclei (Fig. 1). From cycles 8 to 10, the nuclei move to the surface of the embryo, resulting in two obvious macroscopic compartments: the cortical layer, including the nuclei, and the yolk in the centre of the egg (Fig. 1). Not visible on a macroscopic scale, but observable by photobleaching studies, are cytoplasmic islands that are separated from neighbouring islands by semi-permeable barriers (Fig. 1G) (DeLotto et al., 2007; Mavrakis et al., 2009a; Mavrakis et al., 2009b).

Once the Bicoid gradient is established, target genes, such as the *hunchback* and *Kruppel* gap genes, are transcribed at different concentrations of Bicoid and thus at different positions in the embryo (Fig. 2C,D) (Driever and Nusslein-Volhard, 1988a; Driever and Nusslein-Volhard, 1988b; Driever and Nusslein-Volhard, 1989; Driever et al., 1989; Struhl et al., 1989; Hoch et al., 1991; Driever, 2004; Ephrussi and St Johnston, 2004; Nusslein-Volhard, 2004). Bicoid concentration is not the only information read by these target genes. Although altering the gene copy number of *bicoid* induces shifts in the boundaries of target gene expression domains, consistent with a concentration-dependent transcriptional response, the magnitude of these shifts is smaller than would be predicted from a concentration threshold mechanism alone (Driever and Nusslein-Volhard, 1988b; Struhl et al., 1989). Instead, the exact position of each boundary depends on the interactions that occur among the protein products of these target genes, several of which encode transcriptional repressors that are capable of repressing each other (Hoch and Jackle, 1993; Jaeger et al., 2004; Schroeder et al., 2004; Ochoa-Espinosa et al., 2005; Ochoa-Espinosa et al., 2009).

The Bicoid gradient was initially characterised using antibody staining and detection by enzymatic reaction, and images were acquired by bright-field microscopy (Driever and Nusslein-Volhard, 1988a). The concentration of Bicoid in nuclei decreases with the distance from the anterior pole and could be fitted to an exponential decay (Fig. 2E), an observation consistent with the possibility that the gradient arises by diffusion from its local source with spatially uniform degradation. Several models were subsequently proposed to explain the formation of the Bicoid gradient, which we discuss below.

Main models of Bicoid gradient formation

Central to all the models of Bicoid gradient formation is the constant synthesis of Bicoid protein at the anterior pole of the embryo (from an mRNA source that is either point-like or graded), diffusion from its site of production, and its uniform degradation (Houchmandzadeh et al., 2002; Lander et al., 2002; Bergmann et al., 2007; Coppey et al., 2007; Bergmann et al., 2008; Spirov et al., 2009). Within each model, specific assumptions regarding the values of relevant variables (e.g. long or short lifetime) lead to differing interpretations of how the Bicoid gradient forms and whether and when it will be stabilised. The first two models rely solely on production, diffusion (see Box 2) and lifetime (see Box 3).

In mathematical terms, all models of Bicoid gradient formation rely on the following diffusion reaction differential equation, which is written for a semi-infinite one-dimensional system (Rice, 1985):

$$\frac{\partial C(x,t)}{\partial t} = D\frac{\partial^2 C(x,t)}{\partial x^2} - \alpha C(x,t) + j(x,t)\,, \qquad (1)$$

where $C(x,t)$ represents the concentration of Bicoid at time t and position x, D is the diffusion coefficient, α the degradation rate (which is the inverse of the lifetime), and $j(x,t)$ is the source function

Box 2. Diffusion coefficient

When a particle diffuses, its mean displacement is zero because diffusion is an isotropic process (it is uniform in all directions). However, its mean square displacement, which characterises the spread of the particle's position, is a linear function of time. The coefficient of proportionality is called the diffusion coefficient (the unit of which is length^2/time). A larger coefficient reflects a greater spread in position during a given time interval. The significance of an experimentally determined diffusion coefficient depends on how similar the probe used to measure this value is to the actual molecule of interest. For example, an inert probe, such as Dextran, will not localise to nuclei as Bicoid does.

In addition, the temporal window of observation can drastically influence an experimentally determined diffusion coefficient because the effective movement of a probe can include a mixture of mechanistically distinct transport events. On short time scales, such as a few seconds, measurements will reflect the movement of proteins within a cellular compartment. Over the course of minutes, measurements will include the effective diffusion within a compartment together with shuttling of molecules between neighbouring compartments. On the order of hours, molecular transport results from a number of events, including diffusion inside compartments, shuttling between them, and excursions into the deep cytoplasm and possibly the yolk. Moreover, a given time scale is intrinsically linked to a corresponding spatial scale, where short time scales correspond to short spatial scales and long time scales correspond to large spatial scales. Obviously, as the Bicoid gradient forms over a ~2 hour period the relevant diffusion coefficient should be measured on that time scale.

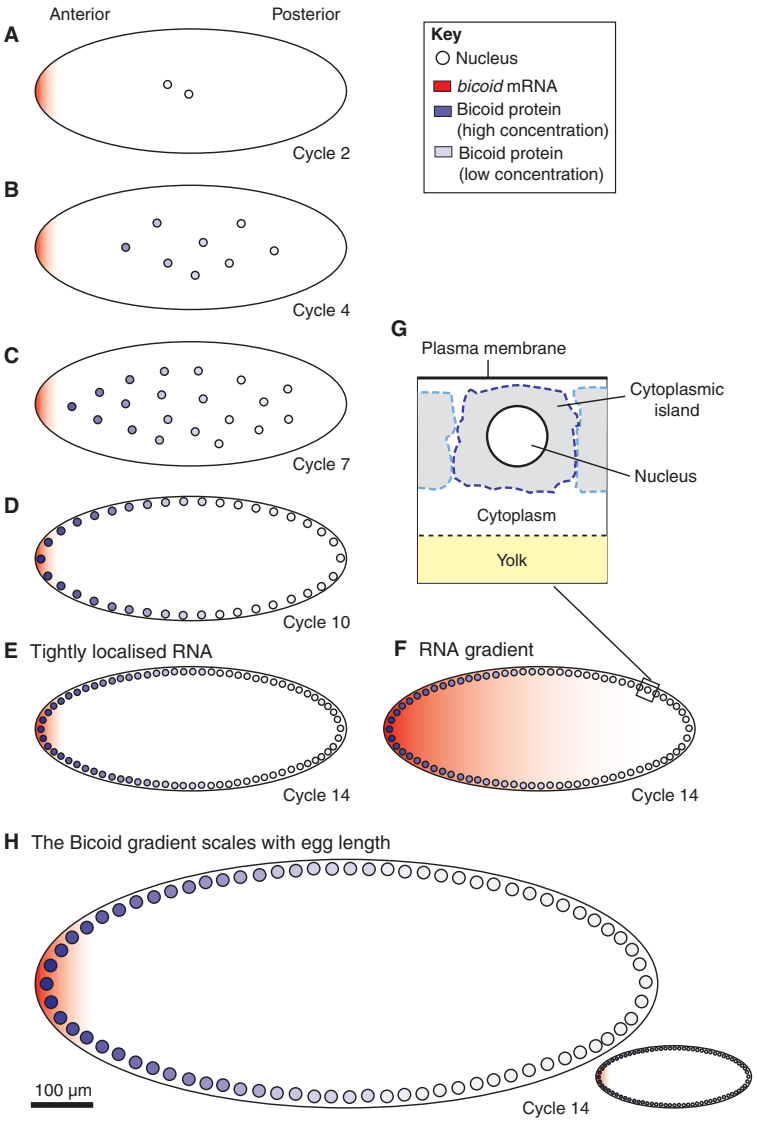

Fig. 1. Schematic of the Bicoid gradient in the syncytial *Drosophila* embryo. (**A-G**) Bicoid, as a transcription factor, accumulates within nuclei during interphase. The nuclear Bicoid gradient, which decreases in concentration with distance from the anterior pole, forms in less than 3 hours in a *Drosophila* embryo that is ~500 μm long (AP axis) and can be observed (B) before nuclei migrate to the surface of the embryo. During the first ~80 minutes (corresponding to cell cycles 1-8), nuclei proliferate in the centre of the embryo (A-C), and then migrate to the surface of the embryo in cycle 9. During the last five cell cycles, nuclei divide at the surface of the embryo (D,E). Nuclei replicate every ~9 minutes during the first nine cell cycles, but this slows to ~20 minutes in cycle 13. Nuclei are ~10 μm in diameter in pre-cycle 14 embryos (A-D) but ~6 μm in cycle 14 (E). The extent to which the mRNA encoding Bicoid, which is initially tightly localised to the anterior pole (A), becomes delocalised is a matter of controversy. Two alternative *bicoid* RNA distributions during cycle 14 are shown in E and F. (G) Illustration of the nucleus and surrounding cytoplasm. (**H**) In species that produce larger or smaller eggs than *Drosophila melanogaster*, the Bicoid gradient scales with egg length.

that describes both the rate and spatial distribution of morphogen production. For a more detailed explanation of this general equation and the following specific models, please see Box 4.

Given the heterogeneity and dynamics of the syncytial embryo, a modelling approach based on partial differential equations might appear to be inappropriate because this approach would need to be complemented by a large set of boundary conditions that describe the exchanges between compartments. Moreover, the parameters D, α and $j(x,t)$ could be different for each compartment, and thus an analytical solution cannot be derived and only numerical simulations would be tractable.

However, the aim of the models presented in this review is to describe the establishment of the gradient over the time and length scales of the embryo without including all the details of the substructures. In this case, the parameters in equation (1) characterise the macroscopic properties of the syncytial embryo and are an average of the reaction and transport events, which include, for example, shuttling of Bicoid between cytoplasmic islands. An explicit formulation of the link between macroscopic parameters and detailed substructures can be obtained through the application of homogenisation routines (Sample and Shvartsman, 2010). The important point when using macroscopic parameters is that great care has to be taken when comparing the experimental values to the parameters of the model as they might not represent directly comparable quantities (see Box 2).

Model 1: the steady-state approximation

The most widely cited model (Wolpert, 1969; Crick, 1970) was formulated before the identification of Bicoid. Wolpert and Crick showed that a simple physical diffusion and reaction model from a localised source can account for most of the phenomenological observations of development known at the time, i.e. that a gradient could be established and naïve tissues patterned over time and length scales (the size of the patterned tissue) that are compatible with diffusion coefficients believed to be relevant for biologically active molecules such as proteins.

The observed exponentially decaying concentration gradient of Bicoid has been taken to mean that the Bicoid gradient arises by local constant protein synthesis, diffusion and spatially uniform degradation (referred to as the SDD model) (Driever and Nusslein-Volhard, 1988a; Houchmandzadeh et al., 2002). If the rate of protein degradation is high (i.e. if its lifetime is short) with respect to the time scale over which the gradient forms, then its distribution approaches a steady state because production is balanced by

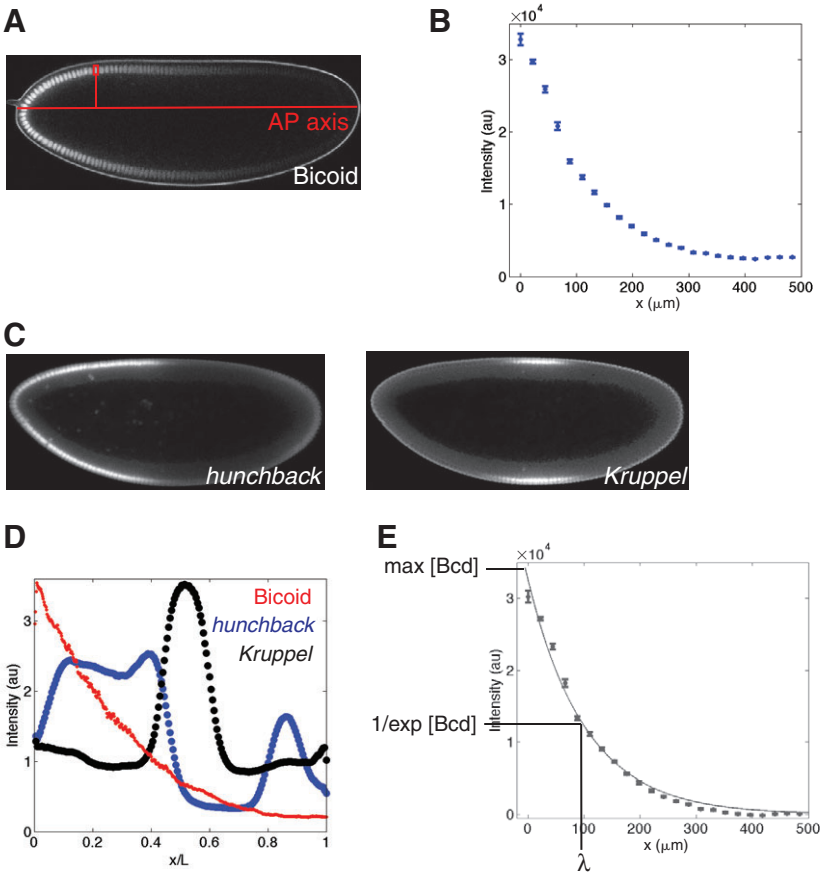

Fig. 2. Bicoid forms a nuclear concentration gradient along the anterior-posterior axis of the *Drosophila* embryo. The Bicoid nuclear concentration gradient provides the *Drosophila* embryo with positional information. (**A**) The Bicoid gradient in cycle 14, visualised by confocal microscopy of a living embryo expressing Venus-Bicoid. Anterior is to the left. The gradient is quantified by sliding a box (red) along the nucleocytoplasmic area and computing the mean pixel intensity within the box. The intensity value is then projected onto the AP axis (red). (**B**) Quantitative information obtained from the embryo in A. The fluorescence intensity (which is proportional to Bicoid concentration) is shown as a function of egg length (x). (**C**) Expression of the Bicoid target genes *hunchback* and *Kruppel* in cycle 14. Anterior is to the left. (**D**) Graph showing the concentration of Bicoid protein (positional information in red) and expression of the target genes *hunchback* and *Kruppel* (blue and black, respectively). x/L is the relative position along the AP axis. (**E**) The length constant, λ, of the Bicoid gradient is obtained by fitting an exponential (red) to the Bicoid intensity profile and computing the position at which the concentration has dropped to 1/exp of the maximal value at the anterior (at x=0). au, arbitrary units.

degradation. The consequence of the balance between synthesis and degradation is that both the total concentration of Bicoid in the embryo and the spatial concentration profile remain stable (Fig. 3A). Mathematically, at steady state, the diffusion reaction equation (1) becomes time independent and allows an exact solution. The concentration of Bicoid at a given position now depends only on the diffusion and lifetime of the protein.

A solution to equation (1) where the source is a point $j(x,t)=Q\delta(x)H(t)$ is obtained by setting the time derivative to zero $\partial C(x,t)/\partial t=0$ (Rice, 1985) so that:

$$C_{ss}(x)=\frac{Q}{\alpha\lambda_{eq}}e^{-\frac{x}{\lambda_{eq}}}, \qquad (2)$$

where Q is the amount of Bicoid being produced at position x=0 at a constant rate, α is the degradation rate, and $\lambda_{eq}=\sqrt{D/\alpha}$ is the length constant (see Box 5) at equilibrium. The overall shape of the gradient is then only defined by the ratio of the diffusion coefficient and the degradation rate.

The notion of steady state originates from the field of mathematics. The steady state is the time-independent asymptotic solution of a differential equation. In real-life experimental conditions, a true steady state cannot be observed as it would require an infinite time of observation. However, most chemical systems relax towards their steady state exponentially quickly. This means that even if the steady state is never reached, an observed quantity can appear to be almost stable, and this stable state will be extremely close to the theoretical steady state. Therefore, an experimental quantity, such as the concentration of a protein, can be described as being at steady state if this quantity is within X% of its steady-state value (known theoretically), where X is a number that is defined arbitrarily.

With respect to the Bicoid gradient, numerous discussions have centred on whether or not the gradient is at steady state. Before asking this question, one should define what steady state means for such an experimentally observed quantity. Furthermore, the Bicoid gradient can appear to be stable without being close to any kind of steady state. Everything depends on what we see as being stable. For example, measurements of the nuclear concentrations of Bicoid may suggest that the total gradient does not change over the last five cell cycles and therefore that the gradient is at steady state. But, as we discuss below, this might or might not be true. It is worth pointing out

Box 3. Protein lifetime and steady state

The lifetime of a protein, that is, its characteristic survival time, sets a limit as to whether and when a steady state is reached. For first-order chemical reactions, such as the uni-molecular degradation scheme $A\xrightarrow{\alpha}\emptyset$, the time evolution of the decaying chemical species is exponential: $[A](t)=[A](t=0)\exp(-\alpha t)$, where $[A](t)$ is the concentration of the chemical species A, and α is the degradation rate (the amount of material being degraded per unit of time).

It is possible to define the lifetime τ as the mean survival time of a particle before it is degraded. For an exponential decay (as above), the lifetime is the inverse of the degradation rate: $\tau=1/\alpha$. Some studies refer to half-life h (the time at which the concentration of the chemical species has dropped to one half of its initial value) rather than to lifetime. The relation between lifetime and half-life is $\tau=h\log(2)$.

Box 4. The synthesis, diffusion and degradation (SDD) equation

The mathematical models presented in this review all rely on partial differential equations that describe Bicoid synthesis, diffusion, degradation and shuttling. The central quantity from which the equations are derived is the concentration of the protein: $C(x,t)$. This is the local concentration of Bicoid at position x at time t and follows equation (1). Below, we explain this equation.

Assuming given time intervals Δt and space intervals Δx, the equation takes the following form:

$$C(x,t+\Delta t) = C(x,t) - \alpha C(x,t)\Delta t + d\left[-C(x,t) + \frac{1}{2}C(x+\Delta x,t) + \frac{1}{2}C(x-\Delta x,t)\right] + j(x,t)\Delta t \ .$$

The right-hand side describes the concentration at position x and at time t plus a small increment Δt. As Δt becomes diminishingly small, the concentration equals the concentration of the protein at the previous time t, $C(x,t)$. During Δt, part of the protein will disappear due to degradation; this is taken into account by the second term of the left-hand side, where $\alpha C(x,t)$ is the amount degraded during time interval Δt. The movement of the protein is described in the next term, which includes three contributions. Owing to diffusion, some of the proteins will leave position x during time interval Δt [the $-C(x,t)$ contribution], and some proteins will have come from the adjacent positions $x+\Delta x$ and $x-\Delta x$. These contributions are adjusted by a factor of one-half because diffusion is isotropic and proteins move to the left or right with equal probability. All these contributions are scaled by a factor d, which is related to the diffusion coefficient D and characterises the probability with which proteins change their position. Finally, the last term describes protein synthesis at time t at position x so that $j(x,t)\Delta t$ is the amount of protein produced by the source during time interval Δt. For a localised source, $j(x,t)$ is zero at all positions outside the source. By reordering the terms of the previous equation, one obtains an equation that describes the rate of change of concentration at any given position x and time t:

$$\frac{C(x,t+\Delta t) - C(x,t)}{\Delta t} = -\alpha C(x,t) + \frac{d(\Delta x)^2}{2\Delta t}\frac{-2C(x,t) + C(x+\Delta x,t) + C(x-\Delta x,t)}{(\Delta x)^2} + j(x,t) \ ,$$

and the continuous diffusion reaction equation (1) is obtained within the limit $\Delta t, \Delta x \rightarrow 0$ assuming that the ratio $d(\Delta x)^2/2\Delta t \equiv D$ is finite.

Box 5. Length constant

The length constant $\langle x \rangle$, or characteristic length, is a quantitative estimate of the spread of a spatial profile (for example, of Bicoid molecules). Mathematically, it is defined as the mean position of a particle that makes up a concentration profile. Let $C(x)$ be a concentration profile of a molecular gradient in which all molecules are independent, meaning they do not interact and therefore do not influence the distribution of each other. The concentration profile can be expressed as:

$$C(x) = N_{tot}p(x) \ ,$$

where $N_{tot} = \int C(x)dx$ is the total number of molecules and $p(x)$ is the probability distribution of one molecule [$\int p(x)dx = 1$ by definition of a probability density].

The characteristic length, explicitly the first moment of a molecule's distribution, is then given by:

$$\langle x \rangle = \int x p(x) dx \ .$$

In the simple case of an exponentially decaying concentration profile $C(x) = \exp(-x/\lambda)$, the characteristic length is the decay length of the exponent. Indeed, in this case, $N_{tot} = \lambda$, $p(x) = 1/\lambda \exp(-x/\lambda)$, and the characteristic length is $\langle x \rangle = 1/\lambda \int \exp(-x/\lambda)dx = \lambda$. In other words, for an exponential profile, the length constant is the position along the AP axis at which the concentration of Bicoid has dropped to 1/exp (about one-third) of its maximal value at the anterior (see also Fig. 1E).

Experimentally, the length constant of the Bicoid gradient was principally obtained by fitting an exponential to the measured intensity profile (using an EGFP-tagged form of Bicoid or antibody staining; see Box 1 for more information) to extract the length constant of the exponent (Fig. 2E). Ideally, the length constant is calculated by the integration of the spatial profile $\langle x \rangle = \int xC(x)dx / \int C(x')dx'$ without assuming an exponentially decaying profile. Note that both methods of computing the length constant strongly depend on estimates of the background level of fluorescence.

that a steady state will be approached at different times at different positions along the AP axis (Bergmann et al., 2007), such that reliable positional information is available earlier closer to the anterior pole.

Model 2: the pre-steady-state hypothesis

Over the timecourse of the syncytial blastoderm (the first 3 hours of *Drosophila* development), the Bicoid gradient may never approach its steady state if the lifetime of Bicoid were long with respect to the time scale over which the gradient forms (Bergmann et al., 2007). The total levels of Bicoid would continue to rise, and target genes would see a continuously changing concentration profile (Fig. 3B). The reading of a dynamic gradient would be expected to cause a gradual posterior shift in the expression boundaries of target genes. Such a shift could be avoided if a precise timing mechanism determined a single point in development when the Bicoid gradient was utilised. In the model proposed by Bergman, such a timing mechanism is postulated to operate in the early syncytial blastoderm, at cycle 10 or 11 (Bergmann et al., 2007).

Mathematically, the solution of equation (1) is now time dependent, meaning that the concentration of the morphogen at a given position is no longer stable but changes with time (Bergmann et al., 2007). As a consequence, both the total concentration and the spatial profile of Bicoid keep changing (Fig. 3B). Both changes become attenuated with increasing time, as can be seen graphically in Fig. 3B, when the curve symbolising the amount of morphogen at a given time asymptotically approaches a limit.

Model 2 is equivalent to model 1, but now the full time-dependent solution of equation (1) is considered (Bergmann et al., 2007):

$$C(x,t) = \frac{Q}{\alpha\lambda_{eq}}\left[e^{-\frac{x}{\lambda_{eq}}} - \frac{e^{-\frac{x}{\lambda_{eq}}}}{2}erfc\left(\frac{2Dt/\lambda_{eq} - x}{\sqrt{4Dt}}\right) - \frac{e^{\frac{x}{\lambda_{eq}}}}{2}erfc\left(\frac{2Dt/\lambda_{eq} + x}{\sqrt{4Dt}}\right)\right] . \quad (3)$$

The length constant λ of the gradient is now dependent on diffusion, degradation and time, and it increases with time (unlike at steady state, where the length constant is time independent and

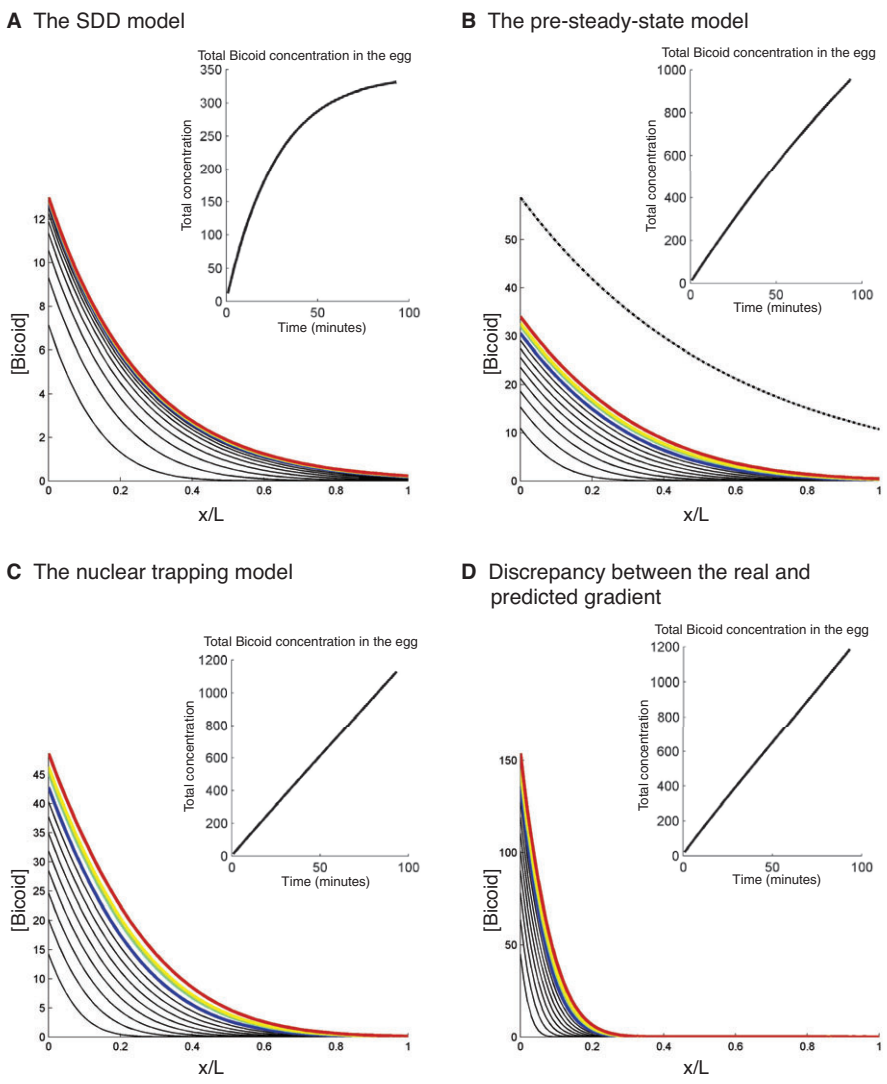

Fig. 3. Time evolution of the Bicoid gradient for the models discussed. Shown are the spatial profile and the total concentration of Bicoid protein as a function of time (inset). x/L, relative egg length; [Bicoid], concentration of Bicoid protein. For all plots, the Bicoid source is assumed to be point-like and constant. The gradient is computed for a one-dimensional infinite space, but these plots have been positioned along an axis of 500 μm, which corresponds to the length of a representative *Drosophila* embryo (see Fig. 2). The black curves illustrate the concentration profile of Bicoid over cell cycles 1-9, and the coloured curves the gradient at cell cycles 10 (blue) to 14 (red); cycle 11 (green), cycle 12 (yellow). (**A**) The synthesis, diffusion and degradation (SDD) model computed for a diffusion coefficient (D) of 10 μm^2/second and a Bicoid lifetime of 20 minutes. The gradient approaches its steady state in less than 100 minutes (see inset). (**B**) The pre-steady-state hypothesis computed for D=5 μm^2/second and a lifetime of 200 minutes. The dashed line indicates the theoretical steady state. At cycle 14 (red curve), the gradient is half the steady-state value. (**C**) The nuclear trapping model computed for D=3 μm^2/second and an infinite lifetime. As in B, the gradient does not approach a steady state (inset). (**D**) Discrepancy between the experimentally observed Bicoid gradient and the gradient computed with $D \approx 0.3$ μm^2/second. If Bicoid diffuses at $D \approx 0.3$ μm^2/second from an anteriorly localised point source, there is no lifetime value for which the theoretically predicted gradient resembles the experimentally observed gradient. With an infinite lifetime, when the length constant of the Bicoid gradient is maximal, the total amount of Bicoid grows linearly as in C (inset).

stable). The shape of the gradient is not a simple exponential and the mathematical expression of the length constant cannot be explicitly given. However, it can be approximated by $\lambda(t)=\sqrt{4Dt}$ for times such that $t<<1/\alpha$, whereas it tends to λ_{eq} for long time periods (Bergmann et al., 2007). At intermediate times, the length constant is always less than the length constant $\lambda_{eff}(t)$ with no degradation (see model 3):

$$\lambda_{eff}(t) = \frac{2}{3\sqrt{\pi}}\lambda(t) \ . \qquad (4)$$

Model 3: the nuclear trapping model

During the period when the Bicoid gradient is being established in the early *Drosophila* embryo, the number of nuclei changes by three orders of magnitude. Because Bicoid, as a transcription factor, accumulates in nuclei, their changing number might affect the gradient locally and/or globally (Lander et al., 2002; Coppey et al., 2007). Such local and global effects have been detected for the gradient of phosphorylated MAPK, which is activated by the receptor tyrosine kinase Torso at the termini of the *Drosophila* embryo (Coppey et al., 2008) and could play a role in both shaping and stabilising the Bicoid gradient. In a simple view, the increasing number of nuclei could balance the increase in the total amount of Bicoid, resulting in a gradient in which nuclear concentrations at a given position remain stable even if Bicoid degradation is too low to balance synthesis or to achieve a stable total concentration. Target genes would read stable nuclear concentrations of Bicoid (as in the steady-state model) even though the total gradient is not at steady state. The most detailed version of this model (Coppey et al., 2007) assumes no degradation of Bicoid (Fig. 3C). It incorporates the constant production of Bicoid at the anterior, diffusion from this source, and the nucleocytoplasmic shuttling of Bicoid. Bicoid is presumed to be bound/immobile when in nuclei and free/diffusible when in the cytoplasm.

Mathematically, a term that describes nucleocytoplasmic shuttling of Bicoid is added to equation (1) (see Box 6). This term does not affect the total concentration of Bicoid in the embryo (which in this particular model depends only on production because there is no degradation) but it does affect the local distribution of Bicoid. As with the previous model, the solution is time dependent, yet the result of nucleocytoplasmic shuttling is that (given the right parameters) a stable, time-independent state is mimicked.

Box 6. Nucleocytoplasmic shuttling

The physical properties of nucleocytoplasmic shuttling are of particular importance as they set the relationship between the concentration of Bicoid in the nuclei, where the developmental decision takes place, and its cytoplasmic concentration, where the gradient is established. The characteristic shuttling time is relatively fast compared with the duration of a nuclear cycle (1 minute versus 8-20 minutes) and allows the nuclear concentration, $N(x,t)$, to be expressed as a simple function of the cytoplasmic concentration $C(x,t)$:

$$N(x,t) = KC(x,t) ,$$

where K is the ratio of nuclear import to nuclear export. As this ratio might change from cycle to cycle, nucleocytoplasmic shuttling would result in a cycle-dependent filter between the cytoplasmic and the nuclear concentration. Nuclear shuttling could also play a non-local role by temporarily sequestering Bicoid proteins and thus decreasing their overall diffusion coefficient. Given physiological parameters, however, the Bicoid gradient is already almost established by nuclear cycle 9 (Coppey et al., 2007), and thus nuclei only play a local role. Under these conditions, the spread of the total concentration gradient $C_{tot}(x,t)=C(x,t)+N(x,t)$ can be approximated by the simple diffusion equation (assuming no degradation):

$$\frac{\partial C_{tot}(x,t)}{\partial t} = D\frac{\partial^2 C_{tot}(x,t)}{\partial x^2} .$$

Eventually, the mathematical quantity that best reflects the experimentally measured Bicoid concentration per nucleus, $n(x,t)$, is obtained by dividing the modelled nuclear concentration by the nuclear density ρ: $n(x,t)=N(x,t)/\rho$. Assuming that the nuclear import k_{in} is proportional to the nuclear density, $n(x,t)$ would be proportional to $C_{tot}(x,t)/1+K$, so that the increase in $C_{tot}(x,t)$ due to continuous production of Bicoid could be balanced by the increase of K.

The varying total Bicoid concentration has the following time-dependent expression (Rice, 1985):

$$C_{tot}(x,t) = \frac{Q}{D}\left(\frac{\lambda(t)}{\sqrt{\pi}}e^{-\frac{x^2}{\lambda(t)^2}} - x\cdot erfc\left(\frac{x}{\lambda(t)}\right)\right), \quad (5)$$

where $\lambda(t)=\sqrt{4Dt}$ is the time-dependent length constant of one molecule forming the gradient of Bicoid produced at the source at time $t=0$. Again, the profile is not a simple exponential. The overall gradient has an effective length constant given by equation (4).

In this model, there is no steady state and total Bicoid concentration increases infinitely (Fig. 3C).

Model 4: a gradient of *bicoid* mRNA

The RNA that encodes the Bicoid protein is synthesized during oogenesis and remains tightly localised to the anterior pole of the egg until fertilisation (St Johnston et al., 1989; St Johnston et al., 1991). At that point, it assumes a more diffuse distribution (Weil et al., 2008) and its translation is presumed to begin. Model 4 incorporates a graded distribution of the *bicoid* RNA source (in contrast to the first three models, see Fig. 1F) (Spirov et al., 2009). How the RNA distribution affects the protein gradient will depend on the distribution of the source RNA and the diffusion/degradation parameters of the protein. If the length constant $\sqrt{D/\alpha}$ of the protein is very low compared with the length scale of the mRNA source (slow diffusion and short lifetime), then Bicoid will accumulate where it is synthesized and the protein distribution will mirror the source RNA distribution (Spirov et al., 2009). However, if $\sqrt{D/\alpha}$ is very large compared with the length scale of the source (if there is no degradation and/or a large diffusion coefficient), then Bicoid will accumulate in the embryo exactly as it would for a point-like source.

As all the mRNA is provided by the mother, if the mRNA diffuses from its initial site at the anterior tip, then it will result in a Gaussian rather than exponential distribution (because there is no production of mRNA). Then, the source term of equation (1) is:

$$j(x,t) = \frac{Q}{\sqrt{2\pi}\sigma}e^{-\frac{x^2}{2\sigma^2}} , \quad (6)$$

where σ is the length constant that characterises the spread of the mRNA Gaussian distribution (we refer to the length constant of the mRNA as $\lambda_{RNA}\equiv\sigma$). The steady-state solution of equation (1) with the source function given in the previous equation can be obtained through a small variation of recently published results (Berezhkovskii et al., 2009):

$$C_{ss}(x) = \frac{Q}{2\alpha\lambda_{eq}}e^{\frac{\sigma^2}{2\lambda_{eq}^2}}\left(e^{\frac{x}{\lambda_{eq}}}erfc\left(\frac{\sigma^2+\lambda_{eq}x}{\sqrt{2}\lambda_{eq}\sigma}\right) + e^{-\frac{x}{\lambda_{eq}}}erfc\left(\frac{\sigma^2-\lambda_{eq}x}{\sqrt{2}\lambda_{eq}\sigma}\right)\right) . \quad (7)$$

As seen from this solution, the overall gradient is not a simple exponential decay and both the length constant σ of the source and the length constant of the protein $\lambda_{eq}=\sqrt{D/\alpha}$ play a role in shaping the gradient. In particular, the length constant of this steady-state gradient is given by (Berezhkovskii et al., 2009):

$$\lambda_{eff} = \lambda_{eq}e^{\frac{\sigma^2}{2\lambda_{eq}^2}}erfc\left(\frac{\sigma}{\sqrt{2}\lambda_{eq}}\right)+\sqrt{\frac{2}{\pi}}\sigma . \quad (8)$$

In conclusion, although all models assume constant production of Bicoid, its diffusion and spatially uniform degradation, and, in one case, nucleocytoplasmic shuttling, the difference in parameter choice (e.g. long or short lifetime) yields Bicoid gradients with very different spatiotemporal characteristics, which would then affect the subsequent interpretation of the gradient by its target genes.

Discussion of the models

The length scale of the gradient and diffusion

The length scale has been the most experimentally measured parameter of the Bicoid gradient (Houchmandzadeh et al., 2002; Crauk and Dostatni, 2005; Gregor et al., 2005; Gregor et al., 2007a; Gregor et al., 2007b; He et al., 2008), as it represents the most obvious quantitative characteristic of the gradient and it is easy to measure both in fixed and living embryos (Fig. 2E). Experimental studies have shown that the length constant λ_{obs} of the exponential fit of the gradient (Fig. 2E, Box 5) is ~100 μm over the 500 μm total egg length.

In all models, the length scale of the Bicoid gradient depends critically on the diffusivity of Bicoid protein. The larger the diffusion coefficient, the more Bicoid reaches positions far from its source. However, the diffusion coefficient that was measured in live embryos is ~0.3 μm^2/second. With this value of diffusivity, models 1-3 cannot explain the experimentally observed length scale of the gradient, as explained below.

The steady-state model (model 1) predicts a length constant of $\lambda_{eq}=\sqrt{D/\alpha}$. Given the low diffusivity of Bicoid protein, for the gradient to achieve 95% of the theoretical steady state after 90 minutes (which corresponds to cycle 10, when nuclear stability is first observed) [$Q(t)=1-e^{t/\tau}$, then $0.95Q=1-e^{90/30}$], the lifetime of Bicoid would have to be less than 30 minutes ($\alpha\geq5.5\times10^{-4}$ seconds). With such numerical values, the maximal length scale of the gradient λ_{eq} would be less than 25 μm, a value far from the observed 100 μm (see Fig. 3D).

The non-stationary models (models 2 and 3), in which the lifetime of Bicoid is assumed to be long or infinite and a steady state is not approached, predict a length constant $\lambda_{eff}(t)=2\sqrt{4Dt/3\sqrt{\pi}}$, which gives a maximal length scale of 35 μm when the considered time is maximal, namely at cycle 14 (t=7200 seconds). At shorter times (after 90 minutes at cycle 10, when nuclear stability is already observed) t=4800 seconds and the length scale is even smaller at $\lambda_{eff}(t)$=28 μm.

For the RNA gradient model (model 4), the situation is different as the length scale of the mRNA source can play a major role in setting the final length scale of the protein gradient. A recent analysis of the mRNA gradient suggests a value of $\lambda_{RNA}/L\approx0.2$ (L being the length of the embryo along the AP axis) at cycle 14 (Spirov et al., 2009), which corresponds to $\lambda_{RNA}\approx100$ μm and is sufficient by itself to explain the length constant of the protein. However, for the formation of the Bicoid gradient, the 2 hours prior to cycle 14 matter the most. During this time, the length scale of the RNA source is ~50 μm (observed for early cycles 9-12) and is probably less than this at earlier times. If the RNA distribution has a length constant of 50 μm, then the gain in the length scale of the protein gradient due to diffusion would be a mere 20 μm, which is insufficient to explain the actual protein distribution.

In conclusion, given the measured length constant and diffusion coefficient, none of the models predicts the gradient as it is actually observed, although an RNA gradient model is potentially more compatible with the observed low diffusion coefficient.

Stability of nuclear concentration

By the time nuclei reach the surface of the embryo during cycle 10 (90 minutes after fertilisation), until cycle 14, the nuclear concentration of Bicoid at a given position remains stable (Gregor et al., 2007a). How can nuclear stability be achieved when nuclei continue proliferating (from cycle 10 to 14 the number of nuclei increases by a factor of 16)?

In the steady-state model (model 1), the total amount of Bicoid in the embryo is fixed at the same time as its spatial concentration profile (Fig. 3A). Under these conditions, stable nuclear concentration can be achieved if nuclear import is proportional to nuclear volume and if the nuclear Bicoid represents only a small fraction of the total pool in the cytoplasm. This is probably the case during cycles 10 through 12, but by cycle 13-14 nuclei begin to represent a significant fraction of the cortical volume.

In the pre-steady-state models (models 2 and 3, Fig. 3B,C), the total concentration of Bicoid in the embryo is predicted to rise and the total gradient continues to change its shape. A balance between total Bicoid levels and the number of nuclei can be achieved only if the total nuclear volume increases linearly with time, assuming that rates of synthesis are constant and accumulation is linear. Although the number of nuclei increases exponentially, their size decreases with each cycle (Gregor et al., 2007a), such that the total increase in nuclear volume is close to linear from cycles 10-13. However, it is unclear how the total amount and spatial distribution of Bicoid protein change over time.

The RNA gradient model (model 4) predicts a short lifetime. In this model, to obtain nuclear stability, the same conditions as those for the steady-state model (model 1) apply: the increasing nuclear volume samples only a small fraction of a constant protein gradient.

In conclusion, to determine which of the models might satisfy the nuclear stability condition we need to know additional parameters, namely the total concentration of Bicoid protein in the egg, its rates of nuclear import and the lifetime of the protein.

Scaling of the gradient

The Bicoid gradient in eggs of different sizes scales such that the length constant is larger in longer eggs (Fig. 1H) (Gregor et al., 2005). It is not obvious how this can be achieved.

One possible mechanism for scaling in model 1, where the length constant is $\lambda_{eq}=\sqrt{D/\alpha}$, is nuclear degradation of Bicoid. If degradation takes place inside (and only inside) nuclei, then the rate of degradation α would be proportional to the nuclear density ρ. This nuclear density is given by $\rho=N/L^2$, where N is the number of nuclei and L the length of the embryo. Because the number of nuclei remains the same in embryos of different lengths, the degradation rate would be inversely proportional to L^2, so that the length constant would be proportional to L, thus achieving scaling.

However, scaling that is mediated by nuclear degradation seems to be in conflict with the stability of the nuclear gradient during successive cleavage divisions if increasing numbers of nuclei increased the overall rate of degradation. The length constant of the gradient $\lambda_{eq}=\sqrt{D/\alpha(\rho)}$ would change at each cycle with respect to the nuclear density. Thus, scaling and stability of the gradient cannot be achieved simultaneously in the steady-state model (model 1).

As noted above, for the gradient to scale, the length constant of the gradient has to be a function of egg length. In the pre-steady-state models, the length constant is time dependent. If the time at which the gradient is utilised were dependent on the length of the embryo, then the gradient would not scale but the pattern of its responses would. To determine whether such a timing mechanism could account for scaling requires a detailed analysis of the developmental timing in different species. As a formal alternative, the embryo could alter the effective diffusion coefficient to scale with egg length. Finally, if the RNA gradient scales with embryo length, then the protein gradient would do so as well. Any potential mechanism(s) responsible for scaling of either the RNA gradient or the effective diffusion coefficient remain unknown.

The unknowns

As discussed above, none of these models can satisfy all of the criteria listed in Box 1. To understand the formation of the Bicoid gradient, we need to add new parameters to these models and to re-evaluate some of the previously measured parameters, as we discuss below.

How does Bicoid move?

All measurements of Bicoid diffusivity so far have resulted in values ($D\approx0.3$ μm^2/second) (Gregor et al., 2007a) that are an order of magnitude too small to explain the length scale of the gradient. This is a problem for all except the RNA gradient model (Spirov et al., 2009), in which the distribution of Bicoid protein is controlled by the as yet unmeasured diffusion of the RNA. So how does Bicoid get to where we see it?

With certainty, these measurements show that there is a fraction of cytoplasmic Bicoid that diffuses slowly. But one cannot exclude several additional uncertainties. (1) There could be another fraction

of cytoplasmic Bicoid that diffuses much faster. All recovery curves from photobleaching experiments start at a level that seems to be much higher than the background, suggesting that a fraction of Bicoid is already re-equilibrated. (2) Fast and effective diffusion events may be visible over longer time scales, perhaps owing to bulk movement or to the 'stirring' of the cytoplasm during cleavage divisions (Hecht et al., 2009). (3) The diffusion coefficient might be much higher in other compartments of the embryo; for example, within the centre of the embryo where diffusion cannot be observed. (4) Bicoid might diffuse faster during early cycles (cycles 1-9), a time during which the Bicoid protein cannot be seen by live imaging, and therefore the diffusion coefficient of Bicoid cannot be measured directly.

How much Bicoid is there?

One prediction of the steady-state model (model 1) is that the total amount of Bicoid in the embryo does not change with time (Fig. 3A). If we knew this value, we could distinguish between the gradient at steady state (constant amount) (Fig. 3A) or at pre-steady state (increasing amount) (Fig. 3B,C). The optical approach (using confocal or two-photon microscopes) only tells us about the surface concentration of Bicoid (which keeps rising and is therefore consistent with the pre-steady-state models), and as we do not know how Bicoid distributes in the various compartments, we cannot infer its total amount in the embryo.

How is Bicoid distributed in each compartment at any stage?

Given the total amount of Bicoid at a given time, we need to know how this amount is partitioned between the physical structures of the embryo. There are several compartments in the syncytial embryo, which are dynamic during the first 3 hours of development when the Bicoid gradient is established (Mavrakis et al., 2009a; Mavrakis et al., 2009b). We do not know the exact volumes of these compartments, except for the nuclei (which are well characterised with respect to their diameter) (Gregor et al., 2007a), and therefore we cannot infer the total amounts of Bicoid in each compartment and have to use relative concentrations. But the geometry and physical properties of these compartments strongly influence the shuttling of Bicoid between them and, as a consequence, the overall transport of Bicoid on the scale of the embryo, as well as its nuclear localisation.

Lifetime

Another way of distinguishing between the steady-state and pre-steady-state models requires us to know the lifetime of Bicoid protein. If the lifetime is short with respect to developmental time scales, then the gradient would approach a steady state (Fig. 3A), whereas with a long or infinite lifetime the gradient would keep changing (Fig. 3B,C).

In addition, the degradation of Bicoid sets a limit to how far the protein can move over a given time. In mathematical terms, lifetime and diffusion control the length scale of the gradient ($\lambda=\sqrt{D\tau}$). The higher the degradation rate, the sharper the profile of the resulting gradient will be.

RNA localisation

Although *bicoid* RNA is tightly bound to the anterior cortex of the developing oocyte during *Drosophila* oogenesis, it has been known for some time that its localisation becomes more diffuse after fertilisation (St Johnston et al., 1989). Part of this displacement involves microtubular transport (Weil et al., 2008). How this dispersion affects the ultimate distribution of Bicoid protein is still a matter of some controversy. Two issues seem important here. First, as the nuclear protein gradient is stable from cycle 10/11, the relevant RNA distribution must precede that point. Second, Bicoid protein is detected in nuclei at the surface and in the centre of the egg. Both these issues point to the importance of measuring RNA distribution early during development, prior to cycle 10 when nuclei are not yet at the surface. So far, published quantifications of RNA have been performed by whole-mount in situ hybridisation, from which only the surface level of *bicoid* mRNA can be reliably measured (Spirov et al., 2009).

Production

Translation of Bicoid protein is assumed to be constant during the first 3 hours of development, when the gradient is established. The major argument supporting constant production is the fact that *bicoid* mRNA is stable for the first 3 hours, before it starts to decay (Surdej and Jacobs-Lorena, 1998). However, the length of the *bicoid* poly(A) tail is dynamic, reaching a maximum length at ~1.5 hours of development, suggesting that Bicoid protein production might not be constant (Salles et al., 1994). In addition, Bicoid protein is undetectable by western blotting in embryos during the first hour of development (Driever and Nusslein-Volhard, 1988a), again suggesting that protein production is not constant. This evidence is indirect, however, and we need a direct measurement of the rate of Bicoid synthesis.

If production turns out to be non-linear, all the models we have discussed (which rely on the constant production assumption) become much more complicated.

Nuclear transport

Nuclear import and export determine the relative cytoplasmic and nuclear concentrations of Bicoid. The experimental observations of this are mainly based on the measured nuclear concentrations of Bicoid. However, the models we discuss predict total Bicoid concentrations. One way to compare the predicted and measured values is by assessing the nuclear transport rates of Bicoid.

At steady state, the relative nuclear and cytoplasmic Bicoid concentrations reveal the import to export ratio, K. If K remains constant over nuclear cycles, then the Bicoid concentration per nucleus reflects the cytoplasmic Bicoid concentration in that these values will differ only by a proportionality constant. By contrast, if K changes with time, then there will be a time-dependent filter between the cytoplasmic and nuclear concentrations.

K can be a function of the nuclear volume, the nuclear surface or the number of nuclei. First, nuclear volume could dictate this ratio if the import rate were controlled by a first-order chemical reaction between cytoplasmic Bicoid proteins and the nuclear binding sites. Second, if the import rate were limited by the diffusive capture of cytoplasmic Bicoid by the nucleus (the time it takes to reach the nuclear surface) or by the number of nuclear pores present on the nuclear membrane, K would be a linear function of the nuclear surface area. Third, if nuclear accumulation were controlled by the non-specific binding of Bicoid to DNA and not by the time needed to enter the nucleus, then K would be proportional to the amount of DNA and thus to the number of nuclei.

The volume of the cytoplasm will be the most relevant physical factor determining the value of K. Potentially, subcompartmentalisation of the cytoplasm could also be a critical feature; for example, if the shuttling of Bicoid within or between cytoplasmic islands reflects an additional set of import-export rates.

When is the gradient utilised?

The transcription of Bicoid target genes has been observed as early as cycle 10 (Knipple et al., 1985; Tautz et al., 1987; Jaeger et al., 2007). At this stage, for certain Bicoid lifetime values, the gradient might be far from its steady state (Fig. 3B,C). If the relevant reading of the Bicoid gradient by target genes occurs at cycle 10, as has been suggested by Bergmann et al. (Bergmann et al., 2007), they would have to read a dynamic gradient and a precise timing mechanism becomes crucial. However, if target genes read the Bicoid gradient only in cycle 14, when it is closer to its steady state, there would be no need for such a mechanism. Therefore, it would be interesting to determine when the Bicoid gradient is actually utilised, or, more precisely, when does the relevant interpretation of the Bicoid gradient occur? For example, Bicoid might induce a low level of *hunchback* and of other gap gene expression at cycle 10, but if the gradient is read continuously in nuclei between cycles 10 and 14, only the high-level response at cycle 14 might be relevant for the next step in patterning and in the establishment of pair-rule gene expression.

The temporal requirement for Bicoid has been tested by shifting a temperature-sensitive *bicoid* allele (called E3) to the restrictive temperature at various developmental stages. Starting at pole-cell formation (cycle 9), *Drosophila* embryos display a high sensitivity to the temperature shift, and this sensitivity lasts until cycle 14, suggesting that Bicoid does matter as early as cycle 9/10 (Frohnhoefer and Nuesslein-Volhard, 1987). In another experiment, anterior cytoplasm (which contains Bicoid) was transferred to hosts of different stages. A strong response (scored by phenotype) was only induced in hosts of ~1.5 hours of age (corresponding approximately to cycle 10), and the strength of the response fell sharply afterwards (Frohnhoefer and Nuesslein-Volhard, 1986).

Lastly, the Bicoid gradient has been perturbed using a microfluidic device, which allows the embryo to be exposed to large temperature differences. Here, the critical time for Bicoid-dependent patterning was found to be between 65 and 100 minutes of development, corresponding to cycles 8-11 (Lucchetta et al., 2005). Together, these experiments support the idea that Bicoid is needed early, around cycle 10/11, consistent with the model proposed by Bergmann et al. (Bergmann et al., 2007). However, if the Bicoid concentration were measured only at cycle 10 and then stably ‘remembered’ during the subsequent proliferation of nuclei, it is hard to explain the tight correlation that is observed between Bicoid and Hunchback levels at cycle 14, because under these circumstances, despite the smooth variation in Bicoid, Hunchback would be expected to show a coarse, patchy distribution in nuclei with similar cycle-10 lineages. The similarly graded distribution of both proteins that is actually observed at cycle 14 (Gregor et al., 2007b) suggests that the Hunchback response continues to be adjusted throughout the syncytial cycles (Gregor et al., 2007b).

Are there different Bicoids?

The models assume the presence of a single Bicoid activity in the embryo, which might not be correct. Western blots demonstrate the presence of differently modified forms of Bicoid in the embryo (Driever and Nusslein-Volhard, 1988a; Ronchi et al., 1993; Janody et al., 2000), and each modification might alter its specific activity. Phosphorylation by the receptor tyrosine kinase Torso affects the transcriptional activity of Bicoid (Ronchi et al., 1993; Janody et al., 2000). Bicoid might be modified by other pathways; removal of a sumoylation enzyme affects its nuclear localisation (Epps and Tanda, 1998), but it is not known whether Bicoid is a direct target of this modification. Bicoid eventually decays, and it is tempting to speculate that this occurs by the ubiquitin proteasome pathway. So even if the total amount of Bicoid were consistent with one or all of the models, the population of Bicoid that matters for providing positional information, i.e. that of the transcriptionally active form, might support a different model. Also, different forms of Bicoid might move at different rates through the embryo. So it will be important to learn more about these modifications and their consequences, and to adjust the models of gradient formation accordingly.

Comparison with other morphogen gradients

For three other morphogen gradients – Dpp and Wg in the fly wing disk (Kicheva et al., 2007) and Fgf8 in the zebrafish embryo (Yu et al., 2009) – the measured key physical parameters, i.e. the diffusion coefficient and the lifetime, are consistent with the SDD model (in which the constant synthesis, diffusion and spatially uniform degradation of the morphogen is assumed). Notably, both Dpp and Wg diffuse at roughly similar rates as Bicoid (<1 μm^2/second), whereas the diffusion coefficient of Fgf8 in the zebrafish embryo is two orders of magnitude higher, similar to the diffusion of a GFP-sized protein in water (Swaminathan et al., 1997; Petrasek and Schwille, 2008). The high Fgf8 diffusion coefficient may reflect properties of the extracellular space in zebrafish (which might, for example, feature fewer binding sites for Fgf8 or low viscosity) or it might be an effect of the measurement method used [fluorescence correlation spectroscopy (FCS)]. In all cases, the lifetimes of these morphogens were found to be short enough for the gradient to approach steady state, given the time available for the formation of these gradients ($\tau_{Fgf8} \approx 30$ minutes, $\tau_{Dpp} \approx 60$ minutes, $\tau_{Wg} \approx 15$ minutes) (Kicheva et al., 2007; Yu et al., 2009).

In the early *Drosophila* embryo, two other morphogen gradients, Dl and MAPK, form within the same environment as the Bicoid gradient, yet the resulting gradients differ in important aspects (DeLotto et al., 2007; Coppey et al., 2008; Kanodia et al., 2009). Although the Bicoid gradient retains both its shape and amplitude (when nuclear Bicoid is observed), the MAPK gradient sharpens with time while retaining its amplitude, and the Dl gradient increases its amplitude and keeps its shape (DeLotto et al., 2007; Coppey et al., 2008; Kanodia et al., 2009). The time at which each morphogen gradient is established is thought to play a role in their different characteristics (Bicoid is assumed to reach its final shape before nuclei reach the surface of the embryo and before nuclei constitute a significant fraction of the embryonic volume), as are the lifetime of the morphogen (the short lifetime of active MAPK) and the spatial extent of the sources that activate Dl (broad source) and MAPK (restricted source) (Kanodia et al., 2009).

Conclusion

Several models have been proposed to account for the establishment of the Bicoid gradient in the *Drosophila* embryo. However, none of those that we have discussed is fully consistent with all available experimental observations; each can only partially account for and explain experimental findings on the Bicoid gradient. Thus, one can assert that there is no consensus on the biophysical mechanisms that underpin Bicoid gradient formation and there is still much to understand about this process. Beyond this fact, we have shown that these simple models raise fundamental questions that highlight the need for new quantitative experiments. It is very likely that this constructive interplay

between models and experiments will soon lead to a unified picture of Bicoid gradient formation. In particular, whether or not future models will be more complex with regard to the number of biophysical parameters that they include, there must be a simple 'coarse-grained' model that can explain the main features of the dynamics of Bicoid and its gradient based on experimentally measured parameters.

Acknowledgements
We are grateful to Stas Shvartsman, Stefano Di Talia, Shawn Little and other members of the E.W. laboratory for helpful suggestions and discussions. M.C. was supported by the Human Frontier Science Program. This work was supported by the Howard Hughes Medical Institute and the NIH. Deposited in PMC for release after 12 months.

Competing interests statement
The authors declare no competing financial interests.

References

Berezhkovskii, A. M., Coppey, M. and Shvartsman, S. Y. (2009). Signaling gradients in cascades of two-state reaction-diffusion systems. *Proc. Natl. Acad. Sci. USA* **106**, 1087-1092.
Bergmann, S., Sandler, O., Sberro, H., Shnider, S., Schejter, E., Shilo, B. Z. and Barkai, N. (2007). Pre-steady-state decoding of the Bicoid morphogen gradient. *PLoS Biol.* **5**, e46.
Bergmann, S., Tamari, Z., Schejter, E., Shilo, B. Z. and Barkai, N. (2008). Re-examining the stability of the Bicoid morphogen gradient. *Cell* **132**, 15-18.
Coppey, M., Berezhkovskii, A. M., Kim, Y., Boettiger, A. N. and Shvartsman, S. Y. (2007). Modeling the bicoid gradient: diffusion and reversible nuclear trapping of a stable protein. *Dev. Biol.* **312**, 623-630.
Coppey, M., Boettiger, A. N., Berezhkovskii, A. M. and Shvartsman, S. Y. (2008). Nuclear trapping shapes the terminal gradient in the Drosophila embryo. *Curr. Biol.* **18**, 915-919.
Crauk, O. and Dostatni, N. (2005). Bicoid determines sharp and precise target gene expression in the Drosophila embryo. *Curr. Biol.* **15**, 1888-1898.
Crick, F. (1970). Diffusion in embryogenesis. *Nature* **225**, 420-422.
DeLotto, R., DeLotto, Y., Steward, R. and Lippincott-Schwartz, J. (2007). Nucleocytoplasmic shuttling mediates the dynamic maintenance of nuclear Dorsal levels during Drosophila embryogenesis. *Development* **134**, 4233-4241.
Driever, W. (2004). The bicoid morphogen papers (II): account from Wolfgang Driever. *Cell* **116**, S7-S9.
Driever, W. and Nusslein-Volhard, C. (1988a). A gradient of bicoid protein in Drosophila embryos. *Cell* **54**, 83-93.
Driever, W. and Nusslein-Volhard, C. (1988b). The bicoid protein determines position in the Drosophila embryo in a concentration-dependent manner. *Cell* **54**, 95-104.
Driever, W. and Nusslein-Volhard, C. (1989). The bicoid protein is a positive regulator of hunchback transcription in the early Drosophila embryo. *Nature* **337**, 138-143.
Driever, W., Thoma, G. and Nusslein-Volhard, C. (1989). Determination of spatial domains of zygotic gene expression in the Drosophila embryo by the affinity of binding sites for the bicoid morphogen. *Nature* **340**, 363-367.
Ephrussi, A. and St Johnston, D. (2004). Seeing is believing: the bicoid morphogen gradient matures. *Cell* **116**, 143-152.
Epps, J. L. and Tanda, S. (1998). The Drosophila semushi mutation blocks nuclear import of bicoid during embryogenesis. *Curr. Biol.* **8**, 1277-1280.
Foe, V. E. and Alberts, B. M. (1983). Studies of nuclear and cytoplasmic behaviour during the five mitotic cycles that precede gastrulation in Drosophila embryogenesis. *J. Cell Sci.* **61**, 31-70.
Frohnhoefer, H. G. and Nuesslein-Volhard, C. (1986). Organization of anterior pattern in the Drosophila embryo by the maternal gene bicoid. *Nature* **324**, 120-125.
Frohnhoefer, H. G. and Nuesslein-Volhard, C. (1987). Maternal genes required for the anterior localization of bicoid in the embryo of Drosophila. *Genes Dev.* **1**, 880-890.
Gierer, A. and Meinhardt, H. (1972). A theory of biological pattern formation. *Kybernetik* **12**, 30-39.
Gregor, T., Bialek, W., de Ruyter van Steveninck, R. R., Tank, D. W. and Wieschaus, E. F. (2005). Diffusion and scaling during early embryonic pattern formation. *Proc. Natl. Acad. Sci. USA* **102**, 18403-18407.
Gregor, T., Wieschaus, E. F., McGregor, A. P., Bialek, W. and Tank, D. W. (2007a). Stability and nuclear dynamics of the bicoid morphogen gradient. *Cell* **130**, 141-152.
Gregor, T., Tank, D. W., Wieschaus, E. F. and Bialek, W. (2007b). Probing the limits to positional information. *Cell* **130**, 153-164.
He, F., Wen, Y., Deng, J., Lin, X., Lu, L. J., Jiao, R. and Ma, J. (2008). Probing intrinsic properties of a robust morphogen gradient in Drosophila. *Dev. Cell* **15**, 558-567.
Hecht, I., Rappel, W. J. and Levine, H. (2009). Determining the scale of the Bicoid morphogen gradient. *Proc. Natl. Acad. Sci. USA* **106**, 1710-1715.
Hoch, M. and Jackle, H. (1993). Transcriptional regulation and spatial patterning in Drosophila. *Curr. Opin. Genet. Dev.* **3**, 566-573.
Hoch, M., Seifert, E. and Jackle, H. (1991). Gene expression mediated by cis-acting sequences of the Kruppel gene in response to the Drosophila morphogens bicoid and hunchback. *EMBO J.* **10**, 2267-2278.
Houchmandzadeh, B., Wieschaus, E. and Leibler, S. (2002). Establishment of developmental precision and proportions in the early Drosophila embryo. *Nature* **415**, 798-802.
Jaeger, J., Surkova, S., Blagov, M., Janssens, H., Kosman, D., Kozlov, K. N., Manu, Myasnikova, E., Vanario-Alonso, C. E., Samsonova, M. et al. (2004). Dynamic control of positional information in the early Drosophila embryo. *Nature* **430**, 368-371.
Jaeger, J., Sharp, D. H. and Reinitz, J. (2007). Known maternal gradients are not sufficient for the establishment of gap domains in Drosophila melanogaster. *Mech. Dev.* **124**, 108-128.
Janody, F., Sturny, R., Catala, F., Desplan, C. and Dostatni, N. (2000). Phosphorylation of bicoid on MAP-kinase sites: contribution to its interaction with the torso pathway. *Development* **127**, 279-289.
Kanodia, J. S., Rikhy, R., Kim, Y., Lund, V. K., DeLotto, R., Lippincott-Schwartz, J. and Shvartsman, S. Y. (2009). Dynamics of the Dorsal morphogen gradient. *Proc. Natl. Acad. Sci. USA* **106**, 21707-21712.
Kicheva, A., Pantazis, P., Bollenbach, T., Kalaidzidis, Y., Bittig, T., Julicher, F. and Gonzalez-Gaitan, M. (2007). Kinetics of morphogen gradient formation. *Science* **315**, 521-525.
Knipple, D. C., Seifert, E., Rosenberg, U. B., Preiss, A. and Jackle, H. (1985). Spatial and temporal patterns of Kruppel gene expression in early Drosophila embryos. *Nature* **317**, 40-44.
Lander, A. D., Nie, Q. and Wan, F. Y. (2002). Do morphogen gradients arise by diffusion? *Dev. Cell* **2**, 785-796.
Lucchetta, E. M., Lee, J. H., Fu, L. A., Patel, N. H. and Ismagilov, R. F. (2005). Dynamics of Drosophila embryonic patterning network perturbed in space and time using microfluidics. *Nature* **434**, 1134-1138.
Manu, Surkova, S., Spirov, A. V., Gursky, V. V., Janssens, H., Kim, A. R., Radulescu, O., Vanario-Alonso, C. E., Sharp, D. H., Samsonova, M. et al. (2009a). Canalization of gene expression and domain shifts in the Drosophila blastoderm by dynamical attractors. *PLoS Comput. Biol.* **5**, e1000303.
Manu, Surkova, S., Spirov, A. V., Gursky, V. V., Janssens, H., Kim, A. R., Radulescu, O., Vanario-Alonso, C. E., Sharp, D. H., Samsonova, M. et al. (2009b). Canalization of gene expression in the Drosophila blastoderm by gap gene cross regulation. *PLoS Biol.* **7**, e1000049.
Mavrakis, M., Rikhy, R. and Lippincott-Schwartz, J. (2009a). Cells within a cell: Insights into cellular architecture and polarization from the organization of the early fly embryo. *Commun. Integr. Biol.* **2**, 313-314.
Mavrakis, M., Rikhy, R. and Lippincott-Schwartz, J. (2009b). Plasma membrane polarity and compartmentalization are established before cellularization in the fly embryo. *Dev. Cell* **16**, 93-104.
Nusslein-Volhard, C. N. (2004). The bicoid morphogen papers (I): account from CNV. *Cell* **116**, S1-S5.
Ochoa-Espinosa, A., Yucel, G., Kaplan, L., Pare, A., Pura, N., Oberstein, A., Papatsenko, D. and Small, S. (2005). The role of binding site cluster strength in Bicoid-dependent patterning in Drosophila. *Proc. Natl. Acad. Sci. USA* **102**, 4960-4965.
Ochoa-Espinosa, A., Yu, D., Tsirigos, A., Struffi, P. and Small, S. (2009). Anterior-posterior positional information in the absence of a strong Bicoid gradient. *Proc. Natl. Acad. Sci. USA* **106**, 3823-3828.
Petrasek, Z. and Schwille, P. (2008). Precise measurement of diffusion coefficients using scanning fluorescence correlation spectroscopy. *Biophys. J.* **94**, 1437-1448.
Rice, S. A. (1985). *Diffusion-Limited Reactions.* Amsterdam: Elsevier.
Ronchi, E., Treisman, J., Dostatni, N., Struhl, G. and Desplan, C. (1993). Down-regulation of the Drosophila morphogen bicoid by the torso receptor-mediated signal transduction cascade. *Cell* **74**, 347-355.
Salles, F. J., Lieberfarb, M. E., Wreden, C., Gergen, J. P. and Strickland, S. (1994). Coordinate initiation of Drosophila development by regulated polyadenylation of maternal messenger RNAs. *Science* **266**, 1996-1999.
Sample, S. and Shvartsman, S. (2010). Multiscale modeling of diffusion in the early Drosophila embryo. *Proc. Natl. Acad. Sci. USA* **107**, 10092-10096.
Schroeder, M. D., Pearce, M., Fak, J., Fan, H., Unnerstall, U., Emberly, E., Rajewsky, N., Siggia, E. D. and Gaul, U. (2004). Transcriptional control in the segmentation gene network of Drosophila. *PLoS Biol.* **2**, E271.
Spirov, A., Fahmy, K., Schneider, M., Frei, E., Noll, M. and Baumgartner, S. (2009). Formation of the bicoid morphogen gradient: an mRNA gradient dictates the protein gradient. *Development* **136**, 605-614.

St Johnston, D., Driever, W., Berleth, T., Richstein, S. and Nusslein-Volhard, C. (1989). Multiple steps in the localization of bicoid RNA to the anterior pole of the Drosophila oocyte. *Development* **107 Suppl**, 13-19.
St Johnston, D., Beuchle, D. and Nusslein-Volhard, C. (1991). Staufen, a gene required to localize maternal RNAs in the Drosophila egg. *Cell* **66**, 51-63.
Struhl, G., Struhl, K. and Macdonald, P. M. (1989). The gradient morphogen bicoid is a concentration-dependent transcriptional activator. *Cell* **57**, 1259-1273.
Surdej, P. and Jacobs-Lorena, M. (1998). Developmental regulation of bicoid mRNA stability is mediated by the first 43 nucleotides of the 3′ untranslated region. *Mol. Cell. Biol.* **18**, 2892-2900.
Swaminathan, R., Hoang, C. P. and Verkman, A. S. (1997). Photobleaching recovery and anisotropy decay of green fluorescent protein GFP-S65T in solution and cells: cytoplasmic viscosity probed by green fluorescent protein translational and rotational diffusion. *Biophys. J.* **72**, 1900-1907.
Tabata, T. and Takei, Y. (2004). Morphogens, their identification and regulation. *Development* **131**, 703-712.
Tautz, D., Lehmann, R., Schnurch, H., Schuh, R., Seifert, E., Kienlin, A., Jones, K. and Jackle, H. (1987). Finger protein of novel structure encoded by hunchback, a second member of the gap class of Drosophila segmentation genes. *Nature* **327**, 383-389.
Turing, A. (1952). The chemical basis of morphogenesis. *Philos. Trans. R. Soc. Lond. B Biol. Sci.* **237**, 37-72.
Weil, T. T., Parton, R., Davis, I. and Gavis, E. R. (2008). Changes in bicoid mRNA anchoring highlight conserved mechanisms during the oocyte-to-embryo transition. *Curr. Biol.* **18**, 1055-1061.
Wolpert, L. (1969). Positional information and the spatial pattern of cellular differentiation. *J. Theor. Biol.* **25**, 1-47.
Yu, S. R., Burkhardt, M., Nowak, M., Ries, J., Petrasek, Z., Scholpp, S., Schwille, P. and Brand, M. (2009). Fgf8 morphogen gradient forms by a source-sink mechanism with freely diffusing molecules. *Nature* **461**, 533-536.